Experimental study of nonlinear solitary waves in two-dimensional dusty plasma

T. E. Sheridan,[1,a)] V. Nosenko,[2,b)] and J. Goree[2,c)]
[1]*Department of Physics and Astronomy, Ohio Northern University, Ada, Ohio 45810, USA*
[2]*Department of Physics and Astronomy, The University of Iowa, Iowa City, Iowa 52242, USA*

The excitation and propagation of solitary waves is studied experimentally in a two-dimensional strongly coupled dusty (complex) plasma. A single layer with ≈ 5000 microspheres (8 μm diam) was suspended in an argon plasma with a neutral gas pressure of 3.0 mTorr. The measured Debye shielding parameter was $\kappa \approx 1.6$, where $\kappa = a/\lambda$ is the ratio of the lattice constant a to the Debye length λ. Nonlinear, planar longitudinal waves were launched by pushing all the particles in a rectangular region at the center of the crystal in the same direction using an 18 W green laser. Compressive solitary waves with density perturbations $\delta n/n_0 \lesssim 0.8$ and widths $\lesssim 5a$ were found to propagate in the forward direction at speeds exceeding the dust acoustic speed. For small amplitude solitary waves, the relations between amplitude, width, and velocity are consistent with those predicted for Korteweg–deVries solitons. Rarefactive perturbations were not observed to evolve into solitary waves. However, oscillatory shocks were seen to move in the backward direction after the laser force was removed. © *2008 American Institute of Physics*. [DOI: 10.1063/1.2955476]

I. INTRODUCTION

Complex (dusty) plasma is a system of microscopic particles immersed in an electron-ion plasma. In laboratory experiments the particles typically acquire a negative charge and are confined by the same electrostatic force that confines electrons. Micrometer-sized particles also feel a significant gravitational force, and so tend to congregate at the lower sheath edge, where the gravitational and electrostatic forces balance. In this case, the particle-particle forces are anisotropic[1] because of ion flow in the sheath. However, both experiment[2] and theory[1] indicate that interactions perpendicular to the ion flow are described by a shielded Coulomb potential (i.e., a Yukawa potential),

$$V(r) = \frac{1}{4\pi\epsilon_0} \frac{Q}{r} e^{-r/\lambda}, \tag{1}$$

where Q is the particle's charge and λ is the Debye length. In analogy with complex fluids, the complex plasma is a "complex" system since the Debye length represents a "*mesoscopic length scale* which necessarily plays a key role in determining the properties of the system."[3]

Under appropriate conditions, it is possible to prepare a two-dimensional (2D) complex plasma. If the particles are monodisperse microspheres, then each has the same mass m and attains nearly the same charge Q. The dust particles may then float in a single layer above a horizontal electrode, where the particle-particle interaction in this system is well described by Eq. (1). The thermodynamic order parameter is

$$\Gamma = \frac{Q^2}{4\pi\epsilon_0 a} \frac{1}{kT_d}, \tag{2}$$

where a is the average interparticle spacing (i.e., the lattice constant for a solid) and T_d is the temperature of the dusty plasma. In the strong-coupling limit $\Gamma \gg 1$, the particles form a two-dimensional solid with a hexagonal lattice.

The relative importance of short- and long-range interactions is determined by the Debye shielding parameter[4]

$$\kappa = \frac{a}{\lambda}. \tag{3}$$

A large system many Debye lengths in extent will behave as a continuum plasma when $\kappa \lesssim 1$.[5,6] In this case there are many particles inside a Debye circle. If the number of particles in a Debye circle is small, $\kappa \gtrsim 1$, then the nearest-neighbor interaction dominates, and the system behaves more like a 2D condensed matter solid. Complex plasma is an interesting experimental system because it is an easily studied 2D system, and because it is possible to vary the shielding parameter κ and thereby move continuously between the nearest-neighbor and plasma regimes.

The 2D solid complex plasma supports both longitudinal (acoustic) and shear waves in the plane of the crystal.[7] For a given value of κ, linear acoustic waves obey the dust-acoustic dispersion relation, as is well-verified by experiment.[8] Due to wave dispersion, a unipolar, longitudinal pulse will broaden as it travels through the lattice. However, if the pulse amplitude is great enough, nonlinear steepening can balance dispersion leading to the formation of a solitary wave (SW), which, in the absence of damping, would have a time-independent profile.

A number of experiments on nonlinear waves in complex plasma have been reported, with a particular interest in compressional waves and shocks. Samsonov *et al.*[9,10] have

---
a)Electronic mail: t-sheridan@onu.edu.
b)Present address: Max-Planck-Institut für Extraterrestrische Physik, D-85741 Garching, Germany.
c)Electronic mail: john-goree@uiowa.edu.

observed dissipative compressional solitary waves and shock melting in a 2D complex plasma crystal for a neutral pressure of 1.8 Pa (13.5 mTorr) using pulsed-wire excitation. Nosenko *et al.*[11] reported evidence for nonlinear effects in compressional pulses, also in a 2D complex plasma crystal, at 15 mTorr using laser excitation powers of 0.66–2.75 W. A number of nonlinear effects were observed, including an increase in pulse speed with amplitude and a nonlinear increase in pulse amplitude in velocity space with the density perturbation. However, the pulses were strongly damped and did not propagate for more than a few pulse widths.

The results of Nosenko *et al.*[11] were modeled by Avinash *et al.*,[4] who derived a Korteweg–deVries (KdV) type equation for nonlinear waves in the two-dimensional Yukawa lattice, and noted that nonlinear effects could be easily overwhelmed by damping in such systems. (Many theoretical treatments of solitary waves in dusty plasma consider three-dimensional continuum models,[12–14] which are not directly applicable to the experiments reported here.)

Properties of single-soliton solutions to the KdV equation are well known.[15] First, the soliton velocity v_s is proportional to its amplitude and is greater than the acoustic wave speed; solitons are supersonic. Second, the soliton width is proportional to the inverse of the square root of the soliton amplitude. That is, faster solitons are "taller" and narrower than slower ones. In addition, solitons are preserved in collisions, and unlike collisions between linear pulses, an overtaking collision between two KdV solitons produces a phase shift[16] such that the overtaken (smaller) soliton is shifted backward in space while the overtaking (larger) soliton is shifted forward.

In traditional three-component plasmas (positive ions, negative ions, and electrons),[15,17] it is known that both compressive and rarefactive (with reference to the positive ion density) solitary waves can exist under appropriate circumstances. The dust particles in complex plasma can be thought of as extremely massive negative ions, so it may be that rarefactive (with respect to the dust) solitary waves will be found in complex plasma. For example, Avinash *et al.*[4] predict the existence of a rarefactive solitary wave whose speed *decreases* as its amplitude *increases*.

In this paper, we extend previous experimental work on nonlinear waves in 2D complex plasma by using significantly lower neutral pressures (3.0 mTorr) than previous studies, so that damping effects are much smaller. We also use very high laser powers (up to 18 W) to produce large, localized perturbations. These initial perturbations evolve into solitary waves, oscillatory shocks, and dust acoustic waves that propagate across the entire complex plasma. Clear evidence of nonlinear behavior is found. Small-amplitude solitary waves have scalings consistent with those expected for KdV solitons. This scaling breaks down for large SW amplitudes, indicating that higher order nonlinearities become important. Large-amplitude rarefactive perturbations were produced, but were not observed to evolve into solitary waves.
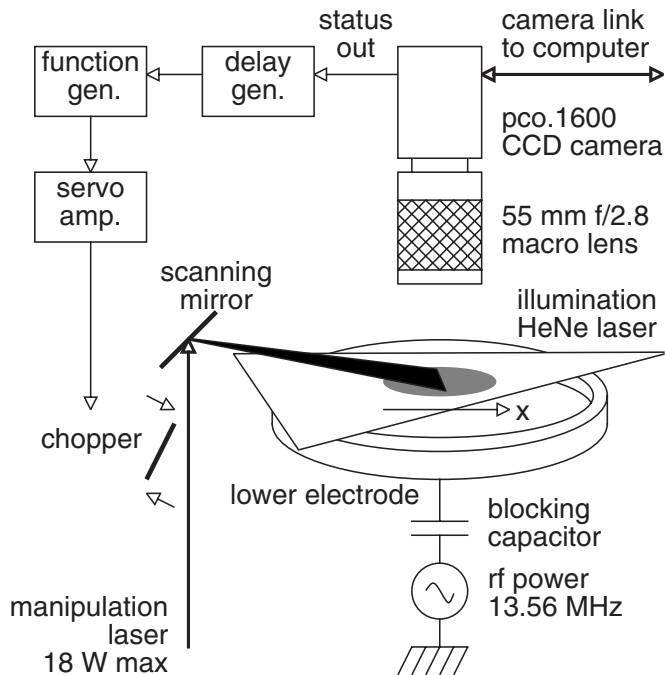

FIG. 1. Experimental schematic. The manipulation laser pushes particles in a rectangular region near the center of the complex plasma disk in the positive *x* direction to launch large-amplitude waves.

II. RESULTS

Experiments were performed in a modified Gaseous Electronics Conference (GEC) reference cell at the University of Iowa (Fig. 1). Neutral argon was introduced into the vacuum vessel at a flow rate of 0.1 sccm and the pressure was stabilized at 3.0 mTorr using a throttle valve on the outlet. A plasma was created using a capacitively coupled rf discharge with a forward power of ≈40 W, a dc self-bias of −96 V, and a peak-to-peak rf voltage of 160 V. A complex plasma crystal was made using particles with a measured[18] diameter of $8.09 \pm 0.18 \ \mu$m. Anomalously large particles were dropped to the electrode, yielding a single-layer suspension. A sideview camera was used to verify that there were never any particles in an incomplete second layer. The primary diagnostic was a 14-bit CCD camera with a resolution of 1600×1200 pixels which captured images at 29.88 frames per second. For these experiments, one pixel corresponded to 0.0382 mm at the crystal. The neutral gas damping coefficient[11] was 0.6 s^{-1}. For this level of damping waves propagate across the entire crystal. Waves were launched by an optical force on the particles[18] due to a 532 nm diode laser with a maximum power of 18 W. Laser excitation provides a well-characterized localized driving force, which, unlike electrical excitation,[9,10] does not globally disturb the electron-ion plasma.

A suspension of ≈5000 particles formed a stable two-dimensional crystal with a hexagonal lattice. However, if very large perturbations were applied, the entire crystal melted and could only be recrystallized by increasing the neutral pressure, which was subsequently lowered back to 3.0 mTorr. The diameter of this crystal was 62 mm, and the average nearest-neighbor distance at the center of the suspen-

sion was $a=0.68$ mm. The crystal was imaged from edge-to-edge in the direction of wave propagation (i.e., the x direction) and was seen to rotate slowly in the counterclockwise direction (viewed from above) at $\omega=0.028$ rad/s (0.27 rev/min). A shear (transverse) wave was excited using the manipulation laser, and the shear wave speed was measured as 6.25 mm/s, while the acoustic (compressional) wave speed was determined to be 24 mm/s. From these values, we compute[19] the Debye shielding parameter $\kappa=1.6$, the Debye length $\lambda=0.43$ mm, and the average particle charge $Q=-14\,900\,e$. In the previous work of Nosenko *et al.*,[11] the largest value of κ attained was 1.45. In the present experiments κ is somewhat larger, and so we expect nonlinear effects to be more prominent.

Compressional pulses were launched by applying a sheet of laser light to the center of the crystal at an oblique angle of 6.1°. The scanning mirror was rastered such that the manipulation laser covered a rectangular stripe (1.8 ± 0.3) mm $\times 32$ mm at the center of the crystal. The laser power at the crystal was modulated (i.e., turned "on" and "off") by a second scanning mirror which chopped the beam in response to a trapezoidal pulse (10% rise and fall times) applied by a function generator. The laser forcing was applied in this way for durations of 0.125, 0.25, and 0.5 s and for laser powers (measured at the laser head) of 17.9, 8.9, 4.5, 2.2 (0.5 s only) and 1.1 W. Using the sideview camera, we verified that particle motion out of the plane of the crystal (i.e., out-of-plane buckling) did not occur. At the highest forcing power, the lattice melted in the region of the laser footprint, but not in the regions where wave properties were characterized. For each set of conditions, 64 frames of data were taken for 10 laser pulses. The laser pulse was synchronized to the video camera, and began at the start of the third video frame. The crystal was allowed to return to a quiescent state between forcing pulses, with a minimum time between pulses of 60 s.

Maps of the particle number density versus time were created by dividing each video frame into 16×16 pixel cells, where 16 pixels=0.61 mm, which is comparable to the lattice constant. Particle positions were then assigned to the grid using area weighting (i.e., cloud-in-cell or CIC).[20] The average particle density in the direction of propagation was then computed by averaging over 17 cells (10.4 mm) in the direction perpendicular to wave propagation. This distance is about 1/3 of the length of the laser footprint, so that edge effects should be minimal. The average of the first two frames was used to establish the initial density profile $n_0(x)$ and the normalized density n/n_0 was computed for frames 3 and onward. Finally, results from all 10 pulses were averaged to give the mean density as a function of position and time. The rotation of the suspension was negligible during the short time interval studied, and no correction was made for this effect.

Figure 2 shows a space-time plot of the density n/n_0 for a laser pulse duration of 0.125 s and a laser power of 17.9 W. This case produced a clean, large-amplitude density perturbation. In this figure, the direction of increasing x corresponds to the direction in which the excitation force acts. A large density solitary wave with an amplitude $n/n_0\approx1.35$ propagates in the forward $(+x)$ direction to the edge of the
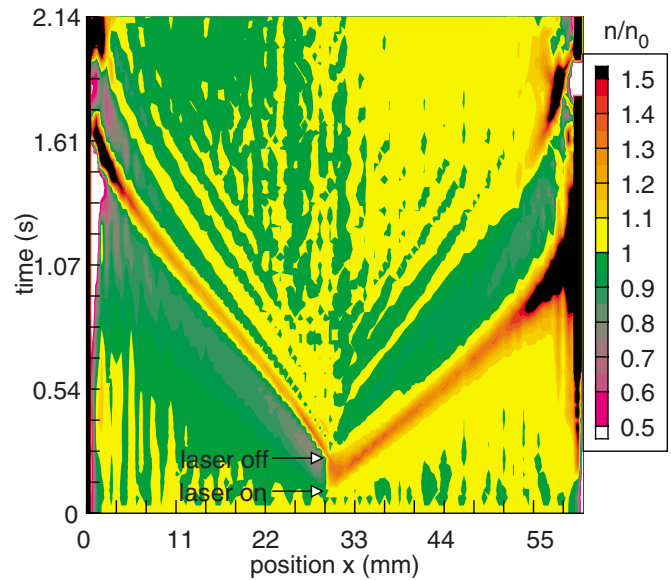

FIG. 2. (Color online) Space-time plot of average complex plasma density n/n_0 for a laser power of 17.9 W and a duration of 0.125 s. The laser excitation force was applied in the positive x direction at $x\approx30$ mm beginning at $t\approx0.1$ s.

crystal at a speed greater than the acoustic speed. A rarefactive perturbation is formed behind the exciting force. However, rather than retaining a constant profile or steepening, as would be expected for a rarefactive SW, this structure is dispersive. Furthermore, even though it is a large perturbation, $n/n_0\approx0.85$, it propagates at the acoustic speed rather than supersonically as would be expected for a solitary wave. We identify this feature as a long-wavelength acoustic wave rather than a solitary wave.

After the laser is turned off, a smaller and narrower compressive perturbation propagates in the backward $(-x)$ direction into the density depleted region. As discussed below, this structure has the features of an oscillatory shock.[21] At around $x=25$ mm and $t=0.5$ s the leading peak of this feature accelerates from 20.5 mm/s, which is below the acoustic speed, to a final speed of 24 mm/s, which is slightly above the dust acoustic speed in this case, as can be seen by the fact that it outpaces the trailing acoustic wave train. This acceleration is consistent with the formation of a supersonic shock. Acoustic waves radiate away from the region where the laser forcing was applied for ≈1 s after the forcing is turned off.

Figure 3 shows the density profile for a number of different times corresponding to the case shown in Fig. 2. Note that the compressional perturbation moves to the right as a coherent unipolar pulse, or solitary wave. The SW amplitude appears to increase near the edge of the crystal because the initial density there is low, so that n/n_0 increases as n_0 decreases. For this reason, data near the edge of the crystal are unreliable. The SW shape is slightly asymmetric, with a more gentle decay at the front and a steeper slope at the back. Such asymmetry cannot be explained by steady-state KdV theory, or by any theory that can be solved in steady state using the Sagdeev (pseudo) potential method.[22] This may be an effect of damping, or it may be that the SW has
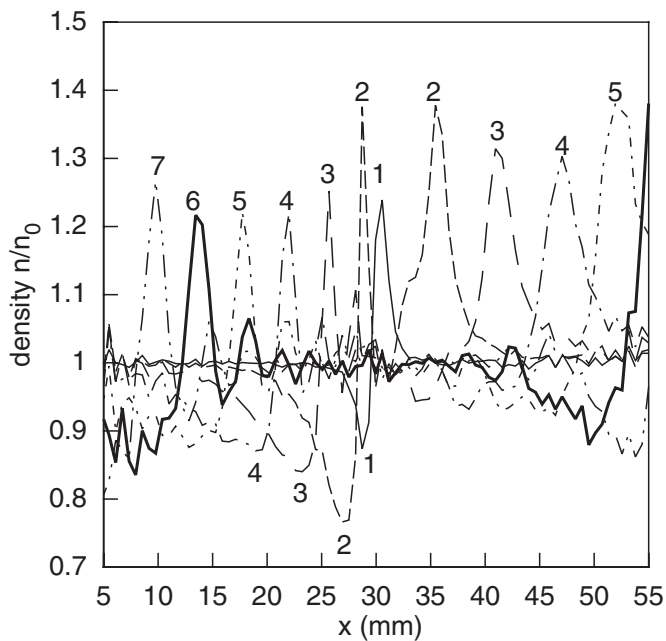
FIG. 3. Average complex plasma density n/n_0 vs position x for times (1) $t=0.133$ s, (2) 0.301 s, (3) 0.469 s, (4) 0.636 s, (5) 0.803 s, (6) 0.971 s, and (7) 1.14 s corresponding to the data in Fig. 2.

FIG. 5. Solitary wave amplitude $\delta n/n_0$ vs laser power for laser pulse durations of 0.125, 0.25, and 0.50 s. There are three points at all laser powers except 2.2 W, where there is a single point.

not attained a steady profile. A large rarefactive perturbation is seen behind the laser footprint. However, rather than steepening into a coherent rarefactive SW, it disperses. After the laser pulse is turned off, the piled-up density behind the laser footprint evolves into a spatially decaying oscillation that propagates to the left into the low density region behind the laser footprint. As seen in line (6) in Fig. 3, the density in front of the leading peak is below the ambient density, while the leading peak is followed by a decaying wave train. These are the characteristics of an oscillatory shock.[21]

A plot of SW amplitude $\delta n/n_0$ and full width at half maximum (FWHM) versus time is shown for the single case of 17.9 W excitation with a 0.125 s duration in Fig. 4. It can be seen that as the solitary wave propagates it becomes wider
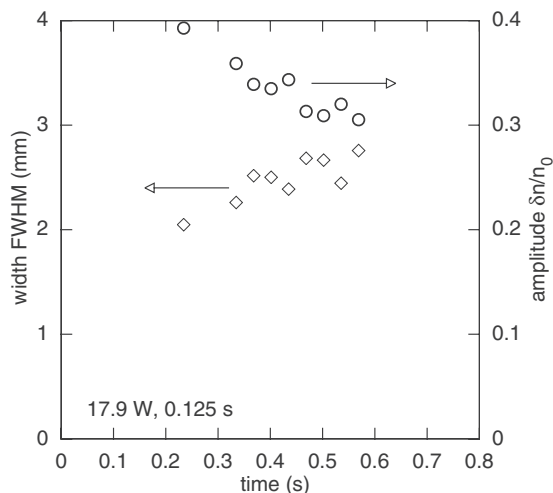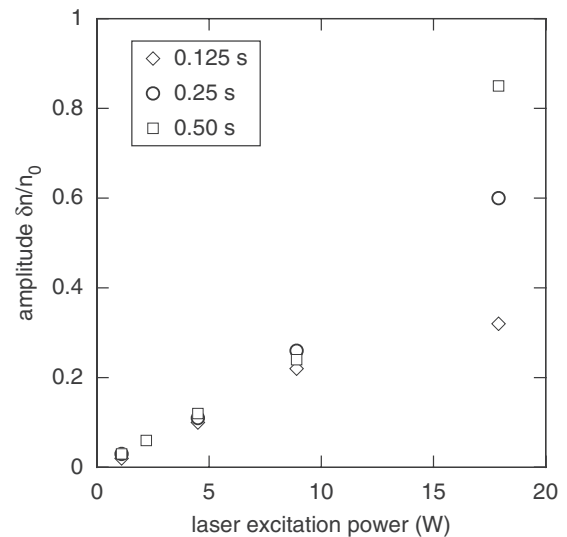

FIG. 4. Full width at half maximum (FWHM) and amplitude $\delta n/n_0$ of the leading solitary wave vs time for 17.9 W laser power and 0.125 s duration.

while its amplitude decreases. This may be due to dispersion or damping. Alternatively, Fig. 4 suggests that the SW may be approaching a constant profile. Data at longer times are not available since the SW reaches the edge of the crystal. Note that the SW is quite narrow, with a FWHM <3 mm, or $\approx 4-5$ lattice constants. That is, the width is comparable to the lattice constant. It is unclear that the KdV equation, which is most often derived using continuum concepts, can be applied to such a narrow solitary wave.

The dependence of the amplitude of the leading compressive SW on laser power and pulse duration is shown in Fig. 5. Note that the SW amplitude increases approximately linearly with laser power below 10 W, indicating that the force exerted on the particles scales linearly with laser power, as expected.[18] There does not appear to be a threshold for exciting waves, unlike the case of negative-potential solitary waves in an electronegative plasma.[17] The effect of pulse duration is significant only for the highest laser power, 17.9 W. For lower laser powers, the amplitude of the resulting solitary wave is effectively independent of pulse duration. This indicates the lattice remains intact for $P \lesssim 9.0$ W. That is, for these powers the effect of the driving force is to push a portion of the lattice away from its equilibrium position until the restoring force balances the driving force, giving a displacement that is independent of pulse duration. However, for $P=17.9$ W, the driving force exceeds the restoring force, breaking the lattice and allowing the density perturbation to continue to increase in time as dust particles are continually pushed onto the back of the perturbation.

A plot of SW speed versus amplitude (i.e., the maximum density perturbation) is shown in Fig. 6. We see an approximately linear increase of speed with amplitude for amplitudes $n/n_0 \lesssim 1.2$. From this plot, the acoustic speed (in the limit of small wave amplitude) is estimated to be 24 mm/s. The SW speed is proportional to amplitude for small amplitudes, indicating nonlinear behavior of the kind predicted from KdV theory. However, for very large solitary waves,
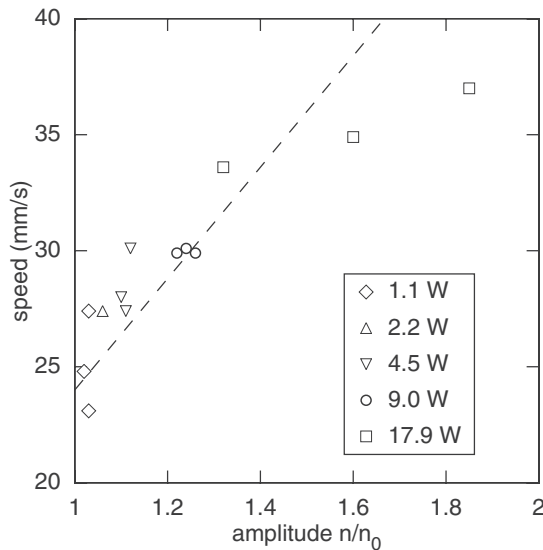
FIG. 6. Solitary wave speed vs amplitude for various laser excitation powers. Note the suppressed zero on the vertical axis. The dashed line shows a linear relation between speed and amplitude for small amplitudes.

the increase in speed with amplitude is sublinear, which may indicate behavior with higher nonlinearities than are included in KdV theory.

A plot of SW width versus amplitude (i.e., the density perturbation) is shown in Fig. 7. Here widths and amplitudes were measured at several times during SW propagation. Widths fall in the range of $2-3.5$ mm, or approximately $3-5$ lattice constants a. Such plots can be used to identify KdV solitons,[15] for which it is expected that width scales like the inverse square root of amplitude. For this scaling, the width will only depend weakly on amplitude, as seen in Fig. 7. Again, for small amplitudes, the measured dependence is consistent with that expected for KdV solitons, while for large SW amplitudes the results are ambiguous.
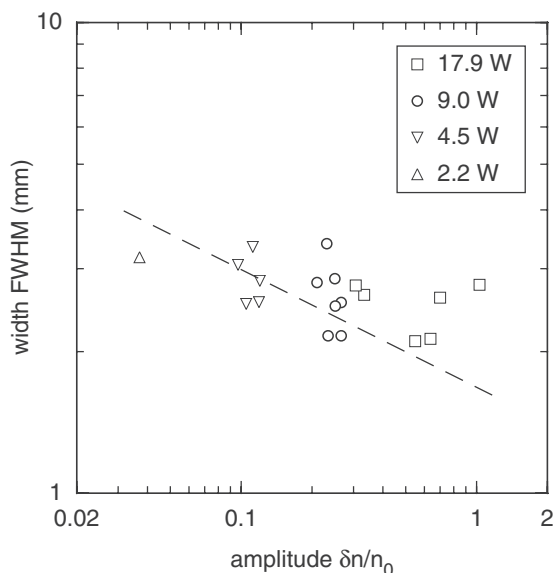

FIG. 7. Solitary wave full width at half maximum (FWHM) vs amplitude $\delta n / n_0$. The dashed line shows the inverse square root scaling predicted for KdV solitons.

III. CONCLUSIONS

We have extended previous experimental work[11] on compressional pulses in two-dimensional complex plasma by using larger driving forces and by working at a lower pressure (3.0 mTorr). In this regime, damping effects are much smaller, allowing nonlinear effects to be more easily observed. The value of the Debye shielding parameter [Eq. (3)] is estimated as $\kappa = 1.6$. Waves were launched using an 18 W green laser, creating large amplitude compressive solitary waves with peak densities of up to $1.8\times$ ambient and Mach numbers over 1.5.

In contrast to previous work,[11] compressive solitary waves were clearly observed to propagate in the forward direction (i.e., in the direction the laser beam pushed) all the way to the edge of the crystal. In fact, one limitation of the current experiment is that the complex plasma is not large enough to determine if the solitary waves have attained steady state. The observed solitary waves are quite narrow, with a width of $\approx 3-5$ times the lattice constant, and it is not clear that they can be accurately described by continuum theory. However, for amplitudes $\delta n / n_0 \lesssim 0.3$, the observed compressional solitary waves had properties consistent with Korteweg–deVries (KdV) solitons, as predicted theoretically.[4] In particular, the SW speed is greater than the acoustic speed and is proportional to amplitude. The dependence of SW width on amplitude is also consistent with the inverse-square root scaling predicted for KdV solitons. When the laser was turned off, an oscillatory shock was seen to propagate in the backward direction and nonlinear evolution from subsonic to supersonic speeds was observed.

Nonlinear steepening in the forward direction was not observed. This may be because the initial perturbation due to the laser is already quite steep and narrow, so that the steady-state solitary wave profile is broader than the initial perturbation profile. That is, the initial perturbation must broaden to become a self-consistent solitary wave. In order to create conditions where steepening can be readily observed, the initial perturbation needs to be wider than the final solitary wave.

The laser force also created a large rarefaction, which was observed to propagate in the backward direction at a speed near, or below, the dust acoustic speed and to disperse. It would be expected that these large perturbations would evolve into rarefactive solitary waves if such objects can exist in this two-dimensional complex plasma. In disagreement with the prediction of Avinash *et al.*,[4] we did not observe the formation of a rarefactive solitary wave.

[1] M. Lampe, G. Joyce, G. Ganguli, and V. Gavrishchaka, Phys. Plasmas **7**, 3851 (2000).
[2] U. Konopka, G. E. Morfill, and L. Ratke, Phys. Rev. Lett. **84**, 891 (2000).
[3] W. M. Gelbart and A. Ben-Shaul, J. Phys. Chem. **100**, 13169 (1996).

[4]K. Avinash, P. Zhu, V. Nosenko, and J. Goree, Phys. Rev. E **68**, 046402 (2003).

[5]T. E. Sheridan, Phys. Plasmas **11**, 5520 (2004).

[6]T. E. Sheridan, Phys. Plasmas **14**, 032108 (2007).

[7]X. Wang, A. Bhattacharjee, and S. Hu, Phys. Rev. Lett. **86**, 2569 (2001).

[8]S. Nunomura, J. Goree, S. Hu, X. Wang, A. Bhattacharjee, and K. Avinash, Phys. Rev. Lett. **89**, 035001 (2002).

[9]D. Samsonov, A. V. Ivlev, R. A. Quinn, G. Morfill, and S. Zhdanov, Phys. Rev. Lett. **88**, 095004 (2002).

[10]D. Samsonov, S. K. Zhdanov, R. A. Quinn, S. I. Popel, and G. E. Morfill, Phys. Rev. Lett. **92**, 255004 (2004).

[11]V. Nosenko, S. Nunomura, and J. Goree, Phys. Rev. Lett. **88**, 215002 (2002).

[12]S. G. Tagare, Phys. Plasmas **4**, 3167 (1997).

[13]A. V. Ivlev and G. Morfill, Phys. Rev. E **63**, 026412 (2001).

[14]F. Verheest, T. Cattaert, and M. A. Hellberg, Phys. Plasmas **12**, 082308 (2005).

[15]K. E. Lonngren, Opt. Quantum Electron. **30**, 615 (1998).

[16]D. W. Aossey, S. R. Skinner, J. L. Cooney, J. E. Williams, M. T. Gavin, D. R. Andersen, and K. E. Lonngren, Phys. Rev. A **45**, 2606 (1992).

[17]T. E. Sheridan and K. E. Lonngren, J. Appl. Phys. **86**, 3520 (1999).

[18]B. Liu, J. Goree, V. Nosenko, and L. Boufendi, Phys. Plasmas **10**, 9 (2003).

[19]S. Nunomura, J. Goree, S. Hu, X. Wang, and A. Bhattacharjee, Phys. Rev. E **65**, 066402 (2002).

[20]C. K. Birdsall and A. B. Langdon, *Plasma Physics via Computer Simulation* (McGraw-Hill, New York, 1985), p. 351.

[21]F. F. Chen, *Introduction to Plasma Physics* (Plenum, New York, 1974), pp. 249–252.

[22]G. Schmidt, *Physics of High Temperature Plasmas* (Academic, New York, 1979), pp. 307–311.